

Cluster-variation method applied in two-site approximation to the Hubbard model at high temperatures

Wai-Ching Ho* and Jeremiah H. Barry

Physics Department, Ohio University, Athens, Ohio 45701

(Received 21 February 1979)

In order to study the origin of metallic magnetism and the metal-insulator transition (Mott transition), the cluster variation method is applied in a two-site approximation to the Hubbard Hamiltonian $H_{\text{Hubbard}} = \sum_{i=1}^{\mathfrak{N}} \sum_{j=1}^{\mathfrak{N}} \sum_{\sigma} t_{ij} c_{i\sigma}^{\dagger} c_{j\sigma} + U \sum_{i=1}^{\mathfrak{N}} n_{i\uparrow} n_{i\downarrow}$, where $c_{i\sigma}^{\dagger}$, $c_{i\sigma}$ are, respectively, the creation and destruction operators of an electron with spin σ (\uparrow or \downarrow) on lattice site i , $n_{i\sigma} = c_{i\sigma}^{\dagger} c_{i\sigma}$, $U > 0$ is the strength of the intrasite Coulomb repulsion between electrons having antiparallel spins, \mathfrak{N} is the total number of sites, and t_{ij} is the "hopping" strength. With the restriction of only nearest-neighbor electron hoppings of strength $-t$ ($t > 0$), and considering the half-filled-band case, both one- and three-dimensional (simple cubic lattice) results are calculated numerically. This is achieved by solving the basic equilibrium equations for the following two-site expectation values: $\langle n_{i\uparrow} n_{i\downarrow} \rangle_0$, $\langle n_{i\uparrow} n_{j\uparrow} \rangle_0$, $\langle n_{i\uparrow} n_{j\downarrow} \rangle_0$, $\langle n_{i\downarrow} n_{j\uparrow} \rangle_0$, $\langle n_{i\downarrow} n_{j\downarrow} \rangle_0$, $\langle c_{i\uparrow}^{\dagger} c_{j\uparrow} \rangle_0$, $\langle c_{i\uparrow}^{\dagger} c_{j\downarrow} \rangle_0$, $\langle c_{i\downarrow}^{\dagger} c_{j\uparrow} \rangle_0$, $\langle c_{i\downarrow}^{\dagger} c_{j\downarrow} \rangle_0$. These expectation values can in turn be used to compute various thermodynamic quantities, e.g., internal energy, entropy, specific heat, etc. For sufficiently large parametric value of U/t , a *high-temperature maximum* in the specific heat is resolved and is identified as an indication of a *gradual* metal-insulator transition. For the simple cubic structure, this high-temperature peak disappears, however, as one decreases the value of U/t to values around or below 15. Also, correlation results strongly suggest that the three-dimensional half-filled-band Hubbard model admits an antiferromagnetic ground state.

I. INTRODUCTION

In 1931, a very successful model of noninteracting electrons was used by Wilson¹ to describe metallic and nonmetallic behaviors of substances. But exceptions do exist, for example, cubic nickel oxide (NiO) should be a metal according to Wilson's model yet actually behaves as an insulator. To take into account the interactions between electrons, Hubbard² introduced a nondegenerate single-energy-band model to represent electronic systems like NiO. In this model, electrons are distributed over localized Wannier sites and can "hop", without changing their spins, from site to site; if two electrons with opposite spins are on the same site then, in the Hubbard model, the energy of the system increases by an amount U . Because of the exclusion principle, electrons with parallel spins are forbidden to occupy the same site. Although this is the simplest model that incorporates both the itinerancy of the electrons and the correlation between electrons on the same site, it is often used to study the origin of metallic magnetism and the metal-insulator transition (Mott transition³). Therefore, solutions to the Hubbard model are highly desirable.

Unfortunately, the mathematics of the Hubbard model is far from trivial, and up to the present, only few exact results are known. For example, Lieb and

Wu⁴ solved the one-dimensional half-filled-band Hubbard model exactly and found an antiferromagnetic ground state with no Mott transition, i.e., the ground state is always insulating—Mott insulator³—for finite U . Following this work, the lowest excited states (spin-wave spectrum⁵) and the magnetic susceptibility at absolute zero temperature⁶ were also determined. However, in order to investigate properties of the Hubbard model at finite temperatures, subsequent authors were forced to resort to various schemes of approximation and reviews on the Hubbard model and these approximation methods appear in the literature.⁷ These methods include, among others, truncation of the Green's-function equations of motion,⁸ series expansion⁹ in the strong- or weak-correlation (large or small U , respectively) limit, and the coherent-potential approximation.¹⁰ In the present investigation, yet another approach is employed, namely, the cluster variation method.¹¹ This method is based upon the variational principle of equilibrium statistical mechanics and lends itself very naturally to systematic approximations. In addition to the present work, Chen¹² has applied the cluster variation method to the half-filled-band Hubbard dimer, dimerized, and uniform Hubbard chains, and recently Chen and Huang¹³ have examined the influence of a uniform magnetic field upon both thermodynamic and correlation properties of Hubbard model systems.

II. THE HUBBARD MODEL

In the Wannier representation, the single-energy-band Hubbard model² takes the form

$$H_{\text{Hubbard}} = \sum_{i=1}^{\mathfrak{N}} \sum_{j=1}^{\mathfrak{N}} \sum_{\sigma} t_{ij} c_{i\sigma}^{\dagger} c_{j\sigma} + U \sum_{i=1}^{\mathfrak{N}} n_{i\uparrow} n_{i\downarrow}, \quad (1)$$

where $c_{i\sigma}^{\dagger}$ and $c_{i\sigma}$ are, respectively, the creation and destruction operators of an electron with spin σ (\uparrow or \downarrow) on the i th Wannier site, $n_{i\sigma} = c_{i\sigma}^{\dagger} c_{i\sigma}$, $U > 0$ is the average Coulomb repulsion energy between two electrons with opposite spins on the same site, t_{ij} is the "hopping" strength [more precisely, t_{ij} is the transfer (overlap) integral between Wannier functions on the i th and j th sites] and \mathfrak{N} is the number of Wannier sites. If the hopping of an electron occurs only between immediately neighboring Wannier sites, or, in other words, the transfer integral t_{ij} in Eq. (1) has the values

$$t_{ij} = \begin{cases} -t, & i, j \text{ nearest neighbors} \\ 0, & \text{otherwise} \end{cases}$$

(i th and j th sites are nearest neighbors) then the Hubbard Hamiltonian (1) becomes

$$H_{\text{H}} = -t \sum_{(i,j)} \sum_{\sigma} (c_{i\sigma}^{\dagger} c_{j\sigma} + c_{j\sigma}^{\dagger} c_{i\sigma}) + U \sum_{i=1}^{\mathfrak{N}} n_{i\uparrow} n_{i\downarrow}, \quad (2)$$

where the sum $\sum_{(i,j)}$ is over all distinct nearest-neighbor pairs. Note that the total width W of the energy band is $4t$.¹⁴ Working in the grand canonical ensemble, one writes, with Eq. (2),

$$\begin{aligned} \mathcal{H}_{\text{H}} &= H_{\text{H}} - \mu N \\ &= H_{\text{H}} - \mu \sum_{i=1}^{\mathfrak{N}} (n_{i\uparrow} + n_{i\downarrow}), \end{aligned} \quad (3)$$

where μ is the chemical potential and N is the electron total-number operator.

As was pointed out in the Introduction, few exact results are known, in general, for the Hubbard model at finite temperatures. But there are some suggestive features resulting from various approximation procedures as well as numerical calculations. For example, in one dimension Shiba and Pincus¹⁴ attempted

to extrapolate the properties of an infinite half-filled-band Hubbard chain by examining the exact results of finite chains and rings of two to six atoms. Using U/W as a parameter, they found that the specific heat has two peaks when $U/W \geq 1$, and associated the high-temperature peak with a gradual metal-insulator transition¹⁵ while the low-temperature peak was attributed to the antiferromagnetic short-range ordering. When U/W becomes small, the two peaks merge into one.

For the three-dimensional case, Langer *et al.*⁸ approximately solved the half-filled-band Hubbard model for a simple-cubic structure by using one-particle Green's functions and established that 0.27 is the demarcation value rather than 1. That is, for $U/W \geq 0.27$, two critical temperatures are found: a Néel order-disorder transition temperature T_N and a higher critical temperature T_M at which the metal-insulator transition occurs. On the other hand, for $U/W < 0.27$, only T_M exists. They, therefore, argued that for a large variety of intermetallic transition-series alloys and oxides, these two critical temperatures with their corresponding specific-heat anomalies, critical fluctuations, etc., should be experimentally observable, although they never calculated these quantities explicitly. More recently, an "exact numerical" solution of the half-filled-band Hubbard model was put forward by Visscher.¹⁶ Even though his numerical procedure does not work in the neighborhood of any singularity, he was able to resolve the high-temperature peak of the specific heat for some values of U/W . He too suggested that this high-temperature peak is due to a gradual metal-insulator transition by observing that the probability of double occupancy, $\langle n_{i\uparrow} n_{i\downarrow} \rangle_0$, decreases rapidly near the peak as the temperature decreases, and this "freezing out" of double occupancy causes a rapid decline in conductivity since the current carriers are extra electrons (doubly occupied sites) and holes (empty sites). However, his calculations are not conclusive enough to indicate any demarcation value of U/W .

In Secs. III–VI, the cluster-variation method in a two-site approximation is applied to the Hubbard Hamiltonian (2) for the half-filled-band case, and some of the findings are compared with the above-mentioned results.

III. APPLICATION OF THE CLUSTER VARIATION METHOD IN TWO-SITE APPROXIMATION

Given the Hubbard Hamiltonian (2), one can express the trial grand free energy in a two-site cluster approximation¹¹ as

$$\begin{aligned} \mathcal{F}_T &= E - \mu N - TS \\ &= \sum_{1 \leq i < j \leq \mathfrak{N}} \text{Tr}_{ij} \rho_T^{(2)}(i,j) \mathcal{H}_{\text{H}} + kT \sum_{i=1}^{\mathfrak{N}} \text{Tr}_i \rho_T^{(1)}(i) \ln \rho_T^{(1)}(i) \\ &\quad + kT \sum_{1 \leq i < j \leq \mathfrak{N}} [\text{Tr}_{ij} \rho_T^{(2)}(i,j) \ln \rho_T^{(2)}(i,j) - \text{Tr}_i \rho_T^{(1)}(i) \ln \rho_T^{(1)}(i) - \text{Tr}_j \rho_T^{(1)}(j) \ln \rho_T^{(1)}(j)] \end{aligned} \quad (4)$$

Since it can be proved that

$$\rho_T^{(2)}(i,j) = \rho_T^{(1)}(i) \otimes \rho_T^{(1)}(j) ,$$

if the i th and j th sites are not nearest neighbors, one has, for such i and j ,

$$\text{Tr}_{i,j} \rho_T^{(2)}(i,j) \ln \rho_T^{(2)}(i,j) = \text{Tr}_i \rho_T^{(1)}(i) \ln \rho_T^{(1)}(i) + \text{Tr}_j \rho_T^{(1)}(j) \ln \rho_T^{(1)}(j) .$$

Using this latter fact, Eq. (4) is simplified so as to become

$$\begin{aligned} \mathcal{F}_T = & \mathcal{N} U \langle n_{i\uparrow} n_{i\downarrow} \rangle - \mathcal{N} \mu \langle n_i \rangle - \mathcal{N} q t (\langle c_{i\uparrow}^\dagger c_{j\uparrow} \rangle + \langle c_{i\downarrow}^\dagger c_{j\downarrow} \rangle) + kT \sum_{i=1}^{\mathcal{N}} \text{Tr}_i \rho_T^{(1)}(i) \ln \rho_T^{(1)}(i) \\ & + kT \sum_{\langle i,j \rangle} [\text{Tr}_{i,j} \rho_T^{(2)}(i,j) \ln \rho_T^{(2)}(i,j) - \text{Tr}_i \rho_T^{(1)}(i) \ln \rho_T^{(1)}(i) - \text{Tr}_j \rho_T^{(1)}(j) \ln \rho_T^{(1)}(j)] , \end{aligned} \quad (5)$$

where q is the lattice coordination number and k is the Boltzmann constant.

It is clear from Eq. (5) that one should attempt at least a two-site cluster approximation, because in a one-site cluster approximation,

$$\langle c_{i\sigma}^\dagger c_{j\sigma} \rangle = \langle c_{i\sigma}^\dagger \rangle \langle c_{j\sigma} \rangle = 0 ,$$

and hence no meaningful results can be derived.

In the present two-site cluster approximation, two reduced trial density matrices are needed, namely, $\rho_T^{(1)}(i)$ and $\rho_T^{(2)}(i,j)$ where the i th and j th sites are nearest neighbors. These matrices are constructed rigorously in Appendix A and are also given in Refs. (23 and 24). It is shown, on the other hand, in Appendix B that the total number of electrons $\sum_{i=1}^{\mathcal{N}} n_{i\sigma}$ with the same spin σ is a constant of motion of the Hubbard Hamiltonian (2). One then concludes that all but the four diagonal elements of $\rho_T^{(1)}(i)$ vanish identically since each off-diagonal element does not preserve this constant of motion, i.e.,

$$\rho_T^{(1)}(i) = \begin{pmatrix} \langle (1 - n_{i\uparrow})(1 - n_{i\downarrow}) \rangle & 0 & 0 & 0 \\ 0 & \langle n_{i\uparrow}(1 - n_{i\downarrow}) \rangle & 0 & 0 \\ 0 & 0 & \langle n_{i\downarrow}(1 - n_{i\uparrow}) \rangle & 0 \\ 0 & 0 & 0 & \langle n_{i\uparrow} n_{i\downarrow} \rangle \end{pmatrix} . \quad (6)$$

For the same reason, most of the 256 elements of $\rho_T^{(2)}(i,j)$ become zero, in fact, only 36 elements remain.

Note that one has assumed, for simplicity, that all Wannier sites are equivalent. This simplification, however, automatically excludes any solution with long-range antiferromagnetic ordering. Note also that the system is not exposed to any external field, so that there is no preference in the direction of electronic spins. One has, therefore, for any i and j ,

$$\begin{aligned} \langle n_{i\sigma} \rangle &= \langle n_{j\sigma} \rangle, \quad \langle n_{i\uparrow} n_{i\downarrow} \rangle = \langle n_{j\uparrow} n_{j\downarrow} \rangle, \quad \text{etc.}, \\ \langle n_{i\uparrow} \rangle &= \langle n_{i\downarrow} \rangle = \frac{1}{2} \langle n_i \rangle, \quad \langle n_{i\uparrow} n_{j\uparrow} \rangle = \langle n_{i\downarrow} n_{j\downarrow} \rangle, \\ \langle n_{i\uparrow} n_{i\downarrow} n_{j\uparrow} \rangle &= \langle n_{i\downarrow} n_{i\uparrow} n_{j\downarrow} \rangle, \quad \langle c_{i\uparrow}^\dagger c_{j\uparrow} \rangle = \langle c_{i\downarrow}^\dagger c_{j\downarrow} \rangle, \\ \langle c_{i\uparrow}^\dagger c_{j\uparrow} n_{i\downarrow} \rangle &= \langle c_{i\downarrow}^\dagger c_{j\downarrow} n_{i\uparrow} \rangle, \\ \langle c_{i\uparrow}^\dagger c_{j\uparrow} n_{j\downarrow} \rangle &= \langle c_{i\downarrow}^\dagger c_{j\downarrow} n_{j\uparrow} \rangle, \\ \langle c_{i\uparrow}^\dagger c_{j\uparrow} n_{i\downarrow} n_{j\downarrow} \rangle &= \langle c_{i\downarrow}^\dagger c_{j\downarrow} n_{i\uparrow} n_{j\uparrow} \rangle . \end{aligned}$$

With these simplifications, the 36 nonvanishing ele-

ments of $\rho_T^{(2)}(i,j)$ can be summarized as follows:

$$\begin{aligned} \rho_{11} &= 1 - 2 \langle n_i \rangle + 2 \langle n_{i\uparrow} n_{i\downarrow} \rangle + 2 \langle n_{i\uparrow} n_{j\uparrow} \rangle \\ &\quad + 2 \langle n_{i\downarrow} n_{j\downarrow} \rangle - 4 \langle n_{i\uparrow} n_{i\downarrow} n_{j\uparrow} \rangle + \langle n_{i\uparrow} n_{i\downarrow} n_{j\uparrow} n_{j\downarrow} \rangle , \\ \rho_{22} &= \rho_{33} = \rho_{55} = \rho_{99} \\ &= \frac{1}{2} \langle n_i \rangle - \langle n_{i\uparrow} n_{i\downarrow} \rangle - \langle n_{i\uparrow} n_{j\uparrow} \rangle - \langle n_{i\downarrow} n_{j\downarrow} \rangle \\ &\quad + 3 \langle n_{i\uparrow} n_{i\downarrow} n_{j\uparrow} \rangle - \langle n_{i\uparrow} n_{i\downarrow} n_{j\uparrow} n_{j\downarrow} \rangle , \\ \rho_{44} &= \rho_{13,13} = \langle n_{i\uparrow} n_{i\downarrow} \rangle - 2 \langle n_{i\uparrow} n_{i\downarrow} n_{j\uparrow} \rangle + \langle n_{i\uparrow} n_{i\downarrow} n_{j\uparrow} n_{j\downarrow} \rangle , \\ \rho_{66} &= \rho_{11,11} = \langle n_{i\uparrow} n_{j\uparrow} \rangle - 2 \langle n_{i\uparrow} n_{i\downarrow} n_{j\uparrow} \rangle + \langle n_{i\uparrow} n_{i\downarrow} n_{j\uparrow} n_{j\downarrow} \rangle , \\ \rho_{77} &= \rho_{10,10} = \langle n_{i\downarrow} n_{j\downarrow} \rangle - 2 \langle n_{i\uparrow} n_{i\downarrow} n_{j\uparrow} \rangle + \langle n_{i\uparrow} n_{i\downarrow} n_{j\uparrow} n_{j\downarrow} \rangle , \\ \rho_{88} &= \rho_{12,12} = \rho_{14,14} = \rho_{15,15} = \langle n_{i\uparrow} n_{i\downarrow} n_{j\uparrow} \rangle - \langle n_{i\uparrow} n_{i\downarrow} n_{j\uparrow} n_{j\downarrow} \rangle , \\ \rho_{16,16} &= \langle n_{i\uparrow} n_{i\downarrow} n_{j\uparrow} n_{j\downarrow} \rangle , \\ \rho_{52} &= \rho_{25} = \rho_{93} = \rho_{39} \\ &= \langle c_{i\uparrow}^\dagger c_{j\uparrow} \rangle - \langle c_{i\uparrow}^\dagger c_{j\uparrow} n_{i\downarrow} \rangle - \langle c_{i\uparrow}^\dagger c_{j\uparrow} n_{j\downarrow} \rangle + \langle c_{i\uparrow}^\dagger c_{j\uparrow} n_{i\downarrow} n_{j\downarrow} \rangle , \\ \rho_{74} &= \rho_{7,13} = -\rho_{10,4} = -\rho_{10,13} = \langle c_{i\uparrow}^\dagger c_{j\uparrow} n_{i\downarrow} \rangle - \langle c_{i\uparrow}^\dagger c_{j\uparrow} n_{i\downarrow} n_{j\downarrow} \rangle \\ \rho_{13,4} &= \rho_{4,13} = \langle c_{i\uparrow}^\dagger c_{i\downarrow}^\dagger c_{j\downarrow} c_{j\uparrow} \rangle , \\ \rho_{10,7} &= \rho_{7,10} = \langle c_{i\uparrow}^\dagger c_{i\downarrow} c_{j\downarrow}^\dagger c_{j\uparrow} \rangle , \\ \rho_{13,7} &= \rho_{47} = -\rho_{13,10} = -\rho_{4,10} = \langle c_{i\uparrow}^\dagger c_{j\uparrow} n_{j\downarrow} \rangle - \langle c_{i\uparrow}^\dagger c_{j\uparrow} n_{i\downarrow} n_{j\downarrow} \rangle \\ \rho_{14,8} &= \rho_{8,14} = \rho_{15,12} = \rho_{12,15} = -\langle c_{i\uparrow}^\dagger c_{j\uparrow} n_{i\downarrow} n_{j\downarrow} \rangle . \end{aligned} \quad (7)$$

From Eqs. (6) and (7), one sees that there are altogether 12 variables (unknown expectation values) under consideration, namely,

$$\begin{aligned} &\langle n_i \rangle, \langle n_{i1}n_{i1} \rangle, \langle n_{i1}n_{j1} \rangle, \langle n_{i1}n_{j1} \rangle, \langle n_{i1}n_{i1}n_{j1} \rangle, \\ &\langle n_{i1}n_{i1}n_{j1}n_{j1} \rangle, \langle c_i^\dagger c_{j1} \rangle, \langle c_i^\dagger c_{j1}n_{i1} \rangle, \\ &\langle c_i^\dagger c_{j1}n_{j1} \rangle, \langle c_i^\dagger c_{j1}n_{i1}n_{j1} \rangle, \langle c_i^\dagger c_i^\dagger c_{j1}c_{j1} \rangle, \langle c_i^\dagger c_i^\dagger c_{j1}^\dagger c_{j1}^\dagger \rangle. \end{aligned}$$

One can also show that these variables are real, since the reduced trial density matrix $\rho_T^{(2)}(i,j)$ is Hermitian, i.e., $\rho_{ml} = \rho_{lm}^*$ ($l, m = 1, 2, \dots, 16$), and $\langle c_i^\dagger c_{j1}n_{i1} \rangle = \langle c_i^\dagger c_{j1}n_{j1} \rangle$ which is shown later [Eq. (15)].

Using elementary column and row operations, the reduced trial density matrix $\rho_T^{(2)}(i,j)$, with its 36 non-vanishing elements given by Eq. (7), can be transformed into a block-diagonal form

$$\rho_T^{(2)}(i,j) \rightarrow \rho_{11} \oplus \Gamma_2 \oplus \Sigma_2 \oplus \rho_{66} \oplus T_4 \oplus \rho_{66} \oplus \Gamma_2 \oplus \Sigma_2 \oplus \rho_{16,16}, \quad (8)$$

where \oplus represents direct sum¹⁷ and Γ_2 , Σ_2 , T_4 are the following square block matrices, respectively:

$$\Gamma_2 = \begin{pmatrix} \rho_{22} & \rho_{52} \\ \rho_{52} & \rho_{22} \end{pmatrix}, \quad \Sigma_2 = \begin{pmatrix} \rho_{88} & \rho_{14,8} \\ \rho_{14,8} & \rho_{88} \end{pmatrix},$$

$$T_4 = \begin{pmatrix} \rho_{77} & \rho_{74} & \rho_{74} & \rho_{10,7} \\ \rho_{13,7} & \rho_{44} & \rho_{13,4} & -\rho_{13,7} \\ \rho_{13,7} & \rho_{13,4} & \rho_{44} & -\rho_{13,7} \\ \rho_{10,7} & -\rho_{74} & -\rho_{74} & \rho_{77} \end{pmatrix}.$$

These square block matrices are readily diagonalized, yielding the following:

$$\Gamma_2 \rightarrow \begin{pmatrix} \rho_{22} - \rho_{52} & 0 \\ 0 & \rho_{22} + \rho_{52} \end{pmatrix},$$

$$\Sigma_2 \rightarrow \begin{pmatrix} \rho_{88} - \rho_{14,8} & 0 \\ 0 & \rho_{88} + \rho_{14,8} \end{pmatrix}, \quad (9)$$

$$T_4 \rightarrow \begin{pmatrix} \rho_{77} - \rho_{10,7} & 2\rho_{74} & 0 & 0 \\ 2\rho_{13,7} & \rho_{44} + \rho_{13,4} & 0 & 0 \\ 0 & 0 & \rho_{44} - \rho_{13,4} & 0 \\ 0 & 0 & 0 & \rho_{77} + \rho_{10,7} \end{pmatrix}.$$

Now it is trivial to write down the eigenvalues of $\rho_T^{(1)}(i)$ according to Eq. (6), i.e.,

$$\begin{aligned} \lambda_1 &= 1 - \langle n_i \rangle + \langle n_{i1}n_{i1} \rangle, \\ \lambda_2 &= \lambda_3 = \frac{1}{2} \langle n_i \rangle - \langle n_{i1}n_{i1} \rangle, \\ \lambda_4 &= \langle n_{i1}n_{i1} \rangle. \end{aligned} \quad (10)$$

On the other hand, using Eqs. (8) and (9), the eigenvalues of $\rho_T^{(2)}(i,j)$ are given as follows:

$$\begin{aligned} \sigma_1 &= \rho_{11}, \quad \sigma_2 = \sigma_{12} = \rho_{22} - \rho_{52}, \\ \sigma_3 &= \sigma_{13} = \rho_{22} + \rho_{52}, \quad \sigma_4 = \sigma_{14} = \rho_{88} - \rho_{14,8}, \\ \sigma_5 &= \sigma_{15} = \rho_{88} + \rho_{14,8}, \quad \sigma_6 = \sigma_{11} = \rho_{66}, \end{aligned} \quad (11)$$

σ_7 and σ_8 are solutions of the equation

$$(\rho_{77} - \rho_{10,7} - \sigma)(\rho_{44} + \rho_{13,4} - \sigma) = 4\rho_{74}\rho_{13,7},$$

and

$$\sigma_9 = \rho_{44} - \rho_{13,4}, \quad \sigma_{10} = \rho_{77} + \rho_{10,7}, \quad \sigma_{16} = \rho_{16,16}.$$

If one defines, for convenience,

$$a \equiv \rho_{77} - \rho_{10,7}, \quad b \equiv \rho_{44} + \rho_{13,4}, \quad c \equiv \rho_{74}\rho_{13,7},$$

then one can write

$$\begin{aligned} \sigma_7 &= \frac{1}{2} \{ (a+b) - [(a-b)^2 + 16c]^{1/2} \}, \\ \sigma_8 &= \frac{1}{2} \{ (a+b) + [(a-b)^2 + 16c]^{1/2} \}. \end{aligned}$$

Note that

$$\sum_{m=1}^4 \lambda_m = \sum_{m=1}^{16} \sigma_m = 1, \quad (12)$$

or in other words, $\rho_T^{(1)}(i)$ and the diagonalized $\rho_T^{(2)}(i,j)$ are normalized as expected.

Now one can perform the trace operations in Eq. (5) readily so that it becomes

$$\mathcal{F}_T = \mathcal{N}U \langle n_{i1}n_{i1} \rangle - \mathcal{N} \mu \langle n_i \rangle - 2\mathcal{N}qt \langle c_i^\dagger c_{j1} \rangle + \mathcal{N}kT \sum_{m=1}^4 \lambda_m \ln \lambda_m + \frac{1}{2} \mathcal{N}qkT \left[\sum_{m=1}^{16} \sigma_m \ln \sigma_m - 2 \sum_{m=1}^4 \lambda_m \ln \lambda_m \right].$$

If one uses x to represent any one of the 12 variables, then Eq. (12) implies that

$$\sum_{m=1}^4 \frac{\partial \lambda_m}{\partial x} = \sum_{m=1}^{16} \frac{\partial \sigma_m}{\partial x} = 0.$$

With this identity and the definition $f_T \equiv \mathcal{F}_T / \mathcal{N}$, the basic equilibrium equations are expressed as

$$\begin{aligned}
0 &= \frac{\partial f_T}{\partial \langle n_i \rangle} = -\mu + kT \sum_{m=1}^4 \ln \lambda_m \frac{\partial \lambda_m}{\partial \langle n_i \rangle} + \frac{1}{2} qkT \left(\sum_{m=1}^{16} \ln \sigma_m \frac{\partial \sigma_m}{\partial \langle n_i \rangle} - 2 \sum_{m=1}^4 \ln \lambda_m \frac{\partial \lambda_m}{\partial \langle n_i \rangle} \right), \\
0 &= \frac{\partial f_T}{\partial \langle n_{i_1} n_{i_1} \rangle} = U + kT \sum_{m=1}^4 \ln \lambda_m \frac{\partial \lambda_m}{\partial \langle n_{i_1} n_{i_1} \rangle} + \frac{1}{2} qkT \left(\sum_{m=1}^{16} \ln \sigma_m \frac{\partial \sigma_m}{\partial \langle n_{i_1} n_{i_1} \rangle} - 2 \sum_{m=1}^4 \ln \lambda_m \frac{\partial \lambda_m}{\partial \langle n_{i_1} n_{i_1} \rangle} \right), \\
0 &= \frac{\partial f_T}{\partial \langle c_{i_1}^\dagger c_{j_1} \rangle} = -2qt + \frac{1}{2} qkT \sum_{m=1}^{16} \ln \sigma_m \frac{\partial \sigma_m}{\partial \langle c_{i_1}^\dagger c_{j_1} \rangle}, \\
0 &= \frac{\partial f_T}{\partial y} = \frac{1}{2} qkT \sum_{m=1}^{16} \ln \sigma_m \frac{\partial \sigma_m}{\partial y},
\end{aligned} \tag{13}$$

where y stands for any one of the remaining nine variables.

Using Eqs. (10) and (11), it is straightforward to rewrite the basic equilibrium equations (13)

$$-\mu + kT \ln \frac{\lambda_2}{\lambda_1} + \frac{1}{2} qkT \left(\ln \frac{\sigma_2 \sigma_3}{\sigma_1^2} - 2 \ln \frac{\lambda_2}{\lambda_1} \right) = 0, \tag{14a}$$

$$\begin{aligned}
U + kT \ln \frac{\lambda_1 \lambda_4}{\lambda_2^2} + \frac{1}{2} qkT \left(\ln \frac{\sigma_1^2 \sigma_9}{\sigma_2^2 \sigma_3^2} + A \ln \sigma_7 \right. \\
\left. + A' \ln \sigma_8 - 2 \ln \frac{\lambda_1 \lambda_4}{\lambda_2^2} \right) = 0,
\end{aligned} \tag{14b}$$

$$qkT \ln \frac{\sigma_1 \sigma_6}{\sigma_2 \sigma_3} = 0, \tag{14c}$$

$$\frac{1}{2} qkT \left(2 \ln \frac{\sigma_1}{\sigma_2 \sigma_3} + A' \ln \sigma_7 + A \ln \sigma_8 + \ln \sigma_{10} \right) = 0, \tag{14d}$$

$$qkT \ln \frac{\sigma_2^3 \sigma_3^3 \sigma_4 \sigma_5}{\sigma_1^2 \sigma_6^2 \sigma_7 \sigma_8 \sigma_9 \sigma_{10}} = 0, \tag{14e}$$

$$\frac{1}{2} qkT \ln \frac{\sigma_1 \sigma_6^2 \sigma_7 \sigma_8 \sigma_9 \sigma_{10} \sigma_{16}}{\sigma_2^2 \sigma_3^2 \sigma_4^2 \sigma_5^2} = 0, \tag{14f}$$

$$-2qt + qkT \ln (\sigma_3 / \sigma_2) = 0, \tag{14g}$$

$$\frac{1}{2} qkT \left(2 \ln \frac{\sigma_2}{\sigma_3} + B \ln \frac{\sigma_7}{\sigma_8} \right) = 0, \tag{14h}$$

$$\frac{1}{2} qkT \left(2 \ln \frac{\sigma_2}{\sigma_3} + C \ln \frac{\sigma_7}{\sigma_8} \right) = 0, \tag{14i}$$

$$\frac{1}{2} qkT \left(2 \ln \frac{\sigma_3 \sigma_4}{\sigma_2 \sigma_5} + (B + C) \ln \frac{\sigma_8}{\sigma_7} \right) = 0, \tag{14j}$$

$$\frac{1}{2} qkT (A \ln \sigma_7 + A' \ln \sigma_8 - \ln \sigma_9) = 0, \tag{14k}$$

$$\frac{1}{2} qkT (-A' \ln \sigma_7 - A \ln \sigma_8 + \ln \sigma_{10}) = 0, \tag{14l}$$

where

$$\begin{aligned}
A &= \frac{1}{2} + \frac{a-b}{2R}, \quad A' = \frac{1}{2} - \frac{a-b}{2R}, \\
B &= -\frac{4}{R} (\langle c_{j_1}^\dagger c_{j_1} n_{j_1} \rangle - \langle c_{i_1}^\dagger c_{j_1} n_{i_1} n_{j_1} \rangle), \\
C &= -\frac{4}{R} (\langle c_{i_1}^\dagger c_{j_1} n_{i_1} \rangle - \langle c_{i_1}^\dagger c_{j_1} n_{i_1} n_{j_1} \rangle),
\end{aligned} \tag{14m}$$

and $R = [(a-b)^2 + 16c]^{1/2}$.

Observe that, by comparing Eqs. (14h) and (14i), $B = C$ for finite temperatures. Thus it follows from Eq. (14m) that

$$\langle c_{i_1}^\dagger c_{j_1} n_{i_1} \rangle = \langle c_{i_1}^\dagger c_{j_1} n_{j_1} \rangle. \tag{15}$$

Also, by substituting Eq. (14l) into Eq. (14d), one has

$$qkT \ln \frac{\sigma_1 \sigma_{10}}{\sigma_2 \sigma_3} = 0,$$

and comparison of this equation with Eq. (14c) yields $\sigma_6 = \sigma_{10}$, or

$$\langle n_{i_1} n_{j_1} \rangle = \langle n_{i_1} n_{j_1} \rangle + \langle c_{i_1}^\dagger c_{i_1} c_{j_1}^\dagger c_{j_1} \rangle. \tag{16}$$

Thus, in thermal equilibrium, two of the 12 variables can be eliminated with the two identities (15) and (16).

IV. EQUILIBRIUM EQUATIONS IN THE HALF-FILLED-BAND CASE

To achieve the half-filled-band condition, one prescribes a chemical potential so that there is on the average one electron per Wannier site, i.e.,

$$\langle n_i \rangle = 1, \tag{17}$$

and then Eqs. (10) reduce to

$$\lambda_1 = \lambda_4 = \langle n_{i_1} n_{i_1} \rangle, \quad \lambda_2 = \lambda_3 = \frac{1}{2} - \langle n_{i_1} n_{i_1} \rangle. \tag{10'}$$

Similarly, using Eqs. (7), and (15)–(17), Eqs. (11)

simplify to

$$\begin{aligned}
 \sigma_1 &= -1 + 2 \langle n_{i1} n_{i1} \rangle + 2 \langle n_{i1} n_{j1} \rangle + 2 \langle n_{i1} n_{j1} \rangle - 4 \langle n_{i1} n_{i1} n_{j1} \rangle + \langle n_{i1} n_{i1} n_{j1} n_{j1} \rangle , \\
 \sigma_2 &= \sigma_{12} = \frac{1}{2} - \langle n_{i1} n_{i1} \rangle - \langle n_{i1} n_{j1} \rangle - \langle n_{i1} n_{j1} \rangle + 3 \langle n_{i1} n_{i1} n_{j1} \rangle - \langle n_{i1} n_{i1} n_{j1} n_{j1} \rangle - \langle c_{i1}^\dagger c_{j1} \rangle + 2 \langle c_{i1}^\dagger c_{j1} n_{i1} \rangle - \langle c_{i1}^\dagger c_{j1} n_{i1} n_{j1} \rangle \\
 \sigma_3 &= \sigma_{13} = \frac{1}{2} - \langle n_{i1} n_{i1} \rangle - \langle n_{i1} n_{j1} \rangle - \langle n_{i1} n_{j1} \rangle + 3 \langle n_{i1} n_{i1} n_{j1} \rangle - \langle n_{i1} n_{i1} n_{j1} n_{j1} \rangle + \langle c_{i1}^\dagger c_{j1} \rangle - 2 \langle c_{i1}^\dagger c_{j1} n_{i1} \rangle + \langle c_{i1}^\dagger c_{j1} n_{i1} n_{j1} \rangle \\
 \sigma_4 &= \sigma_{14} = \langle n_{i1} n_{i1} n_{j1} \rangle - \langle n_{i1} n_{i1} n_{j1} n_{j1} \rangle + \langle c_{i1}^\dagger c_{j1} n_{i1} n_{j1} \rangle , \\
 \sigma_5 &= \sigma_{15} = \langle n_{i1} n_{i1} n_{j1} \rangle - \langle n_{i1} n_{i1} n_{j1} n_{j1} \rangle - \langle c_{i1}^\dagger c_{j1} n_{i1} n_{j1} \rangle , \\
 \sigma_6 &= \sigma_{10} = \sigma_{11} = \langle n_{i1} n_{j1} \rangle - 2 \langle n_{i1} n_{i1} n_{j1} \rangle + \langle n_{i1} n_{i1} n_{j1} n_{j1} \rangle , \\
 \sigma_7 &= \frac{1}{2} \{ (a+b) - [(a-b)^2 + 16c]^{1/2} \} , \\
 \sigma_8 &= \frac{1}{2} \{ (a+b) + [(a-b)^2 + 16c]^{1/2} \} , \\
 \sigma_9 &= \langle n_{i1} n_{i1} \rangle - 2 \langle n_{i1} n_{i1} n_{j1} \rangle + \langle n_{i1} n_{i1} n_{j1} n_{j1} \rangle - \langle c_{i1}^\dagger c_{i1}^\dagger c_{j1} c_{j1} \rangle , \\
 \sigma_{16} &= \langle n_{i1} n_{i1} n_{j1} n_{j1} \rangle ,
 \end{aligned} \tag{11'}$$

where

$$\begin{aligned}
 a &= 2 \langle n_{i1} n_{j1} \rangle - \langle n_{i1} n_{j1} \rangle - 2 \langle n_{i1} n_{i1} n_{j1} \rangle + \langle n_{i1} n_{i1} n_{j1} n_{j1} \rangle , \\
 b &= \langle n_{i1} n_{i1} \rangle - 2 \langle n_{i1} n_{i1} n_{j1} \rangle + \langle n_{i1} n_{i1} n_{j1} n_{j1} \rangle + \langle c_{i1}^\dagger c_{i1}^\dagger c_{j1} c_{j1} \rangle , \\
 c &= (\langle c_{i1}^\dagger c_{j1} n_{i1} \rangle - \langle c_{i1}^\dagger c_{j1} n_{i1} n_{j1} \rangle)^2 .
 \end{aligned}$$

Note that the number of variables changes from 12 to 9 because of Eqs. (15)–(17); thus some of the 12 basic equilibrium equations (14a)–(14l) are redundant, for example, Eq. (14a) can be used to calculate the prescribed value of the chemical potential. Therefore, one has to eliminate the redundancy by choosing suitable linear combinations of the 12 basic equilibrium equations; in fact, the following nine equations are used for numerical purposes:

$$\frac{U/t}{kT/t} + 2 \ln \frac{\lambda_1}{\lambda_2} + q \left(\ln \frac{\sigma_1 \sigma_9}{\sigma_2 \sigma_3} - 2 \ln \frac{\lambda_1}{\lambda_2} \right) = 0 , \tag{18a}$$

$$\ln \frac{\sigma_1 \sigma_6}{\sigma_2 \sigma_3} = 0 , \tag{18b}$$

$$\ln \frac{\sigma_2^3 \sigma_3^3 \sigma_4 \sigma_5}{\sigma_1^2 \sigma_6^3 \sigma_7 \sigma_8 \sigma_9} = 0 , \tag{18c}$$

$$\ln \frac{\sigma_1 \sigma_6^3 \sigma_7 \sigma_8 \sigma_9 \sigma_{16}}{\sigma_2^2 \sigma_3^2 \sigma_4^2 \sigma_5^2} = 0 , \tag{18d}$$

$$-\frac{2}{kT/t} + \ln \frac{\sigma_3}{\sigma_2} = 0 , \tag{18e}$$

$$2 \ln \frac{\sigma_2}{\sigma_3} + B \ln \frac{\sigma_7}{\sigma_8} = 0 , \tag{18f}$$

$$\ln \frac{\sigma_2 \sigma_4}{\sigma_3 \sigma_5} = 0 , \tag{18g}$$

$$\ln \frac{\sigma_7 \sigma_8}{\sigma_6 \sigma_9} = 0 , \tag{18h}$$

$$\frac{a-b}{[(a-b)^2 + 16c]^{1/2}} \ln \frac{\sigma_7}{\sigma_8} + \ln \frac{\sigma_{10}}{\sigma_9} = 0 . \tag{18i}$$

Here, one has a set of nine coupled algebraic and transcendental equations (18a)–(18i) with nine variables, namely,

$$\begin{aligned}
 &\langle n_{i1} n_{i1} \rangle, \quad \langle n_{i1} n_{j1} \rangle, \quad \langle n_{i1} n_{j1} \rangle , \\
 &\langle n_{i1} n_{i1} n_{j1} \rangle, \quad \langle n_{i1} n_{i1} n_{j1} n_{j1} \rangle, \\
 &\langle c_{i1}^\dagger c_{j1} \rangle, \quad \langle c_{i1}^\dagger c_{j1} n_{i1} \rangle , \\
 &\langle c_{i1}^\dagger c_{j1} n_{i1} n_{j1} \rangle, \quad \langle c_{i1}^\dagger c_{i1}^\dagger c_{j1} c_{j1} \rangle .
 \end{aligned}$$

This, obviously, is a problem for the machine!

V. NUMERICAL CALCULATIONS AND RESULTS

In the present research, a computer program called MINMAX¹⁸ is employed to solve the nine nonlinear equations (18a)–(18i) at each temperature. Given an initial guess of the values of the variables (not too far away from the actual solution), MINMAX, using some iteration procedures, manipulates the variables to make the nonlinear equations hold simultaneously to within a small predefined error (the numerical error permitted here is 10^{-10}). Towards such a goal one realizes that, at high temperatures, the mean-field results, i.e.,

$$\begin{aligned}
 \langle n_{i1} n_{i1} \rangle &= \langle n_{i1} \rangle \langle n_{i1} \rangle , \\
 \langle c_{i1}^\dagger c_{j1} \rangle &= \langle c_{i1}^\dagger \rangle \langle c_{j1} \rangle, \quad \text{etc.},
 \end{aligned}$$

should be reasonably close to the equilibrium values.

Thus, for each parameteric value of q and U/t , one commences the numerical calculation at a high temperature with the following initial guesses:

$$\begin{aligned} \langle n_{i\uparrow} n_{i\downarrow} \rangle &= \langle n_{i\uparrow} n_{j\uparrow} \rangle = \langle n_{i\uparrow} n_{j\downarrow} \rangle = \frac{1}{4} , \\ \langle n_{i\uparrow} n_{i\downarrow} n_{j\uparrow} \rangle &= \frac{1}{8} , \quad \langle n_{i\uparrow} n_{i\downarrow} n_{j\uparrow} n_{j\downarrow} \rangle = \frac{1}{16} , \\ \langle c_{i\uparrow}^\dagger c_{j\uparrow} \rangle &= \langle c_{i\uparrow}^\dagger c_{j\uparrow} n_{i\downarrow} \rangle = \langle c_{i\uparrow}^\dagger c_{j\uparrow} n_{i\downarrow} n_{j\downarrow} \rangle \\ &= \langle c_{i\uparrow}^\dagger c_{i\downarrow}^\dagger c_{j\downarrow} c_{j\uparrow} \rangle = 0 . \end{aligned}$$

If the program gives convergence, then the new equilibrium values are taken as the initial guess for calculation at a lower temperature, and so forth. All these calculations are done using an IBM system/360 Model 44 digital computer with a memory of 64K words. A typical run consists of six to seven 900-second jobs covering temperatures from $kT/t = 10^8$ to $kT/t \approx 1$, and yields about 50–60 data points. Each data point contains the values of nine equilibrium expectation values

$$\begin{aligned} \langle n_{i\uparrow} n_{i\downarrow} \rangle_0, \quad \langle n_{i\uparrow} n_{j\uparrow} \rangle_0, \quad \langle n_{i\uparrow} n_{j\downarrow} \rangle_0 , \\ \langle n_{i\uparrow} n_{i\downarrow} n_{j\uparrow} \rangle_0, \quad \langle n_{i\uparrow} n_{i\downarrow} n_{j\uparrow} n_{j\downarrow} \rangle_0 , \\ \langle c_{i\uparrow}^\dagger c_{j\uparrow} \rangle_0, \quad \langle c_{i\uparrow}^\dagger c_{j\uparrow} n_{i\downarrow} \rangle_0 , \\ \langle c_{i\uparrow}^\dagger c_{j\uparrow} n_{i\downarrow} n_{j\downarrow} \rangle_0, \quad \langle c_{i\uparrow}^\dagger c_{i\downarrow}^\dagger c_{j\downarrow} c_{j\uparrow} \rangle_0 , \end{aligned} \quad (19)$$

where the subscript "0" is used to denote stable thermodynamic equilibrium quantities.

Using the equilibrium expectation values (19), thermodynamic quantities can be computed easily, for example, the internal energy E is given by

$$\frac{E}{\mathfrak{N}t} = \frac{U}{t} \langle n_{i\uparrow} n_{i\downarrow} \rangle_0 - 2q \langle c_{i\uparrow}^\dagger c_{j\uparrow} \rangle_0 ,$$

the entropy S ,

$$\begin{aligned} \frac{S}{\mathfrak{N}k} = & - \sum_{m=1}^4 \lambda_m \ln \lambda_m \\ & - \frac{1}{2} q \left[\sum_{m=1}^{16} \sigma_m \ln \sigma_m - 2 \sum_{m=1}^4 \lambda_m \ln \lambda_m \right] , \end{aligned}$$

and the prescribed value of the chemical potential μ ,

$$\frac{\mu}{t} = \frac{kT}{t} \ln \frac{\lambda_2}{\lambda_1} + \frac{1}{2} q \frac{kT}{t} \left[\ln \frac{\sigma_2 \sigma_3}{\sigma_1^2} - 2 \ln \frac{\lambda_2}{\lambda_1} \right] .$$

One can also differentiate the entropy data numerically to get the heat capacity at constant volume, since

$$C_V = T \left(\frac{\partial S}{\partial T} \right)_{\mu, V} .$$

To certify the accuracy of the present calculations, one first examines the computed numerical values of μ , since according to a rigorous theorem,¹⁹ $\mu = \frac{1}{2} U$ in

the half-filled-band case. One indeed finds that the above equality is valid with a relative error of about $\pm 0.008\%$ or 0.00002% for small (~ 1) or large (~ 10 – 100) values of U/t , respectively. On the other hand, since the only quantity involving lattice dimensionality in the above solution is the lattice coordination number q , numerical calculations for half-filled-band Hubbard models of different dimensions can be carried out readily by using appropriate values of the lattice coordination number²⁰ q . Thus a further check of the solution is to perform calculations on the infinite half-filled-band uniform Hubbard chain (i.e., $q=2$) and compare the results with those of Shiba and Pincus.¹⁴ The findings, with $U/t=8$, are displayed in Figs. 1, 2, and 3. The results, in general, are in good agreement, since it is clear that as the number of atoms increases, the thermodynamic quantities also increase. The present calculation, however, is terminated after the appearance of the high-temperature peak in the specific-heat curve for two reasons, namely, the low-temperature anomaly, corresponding to a Néel transition, has been excluded from the present solution, and the

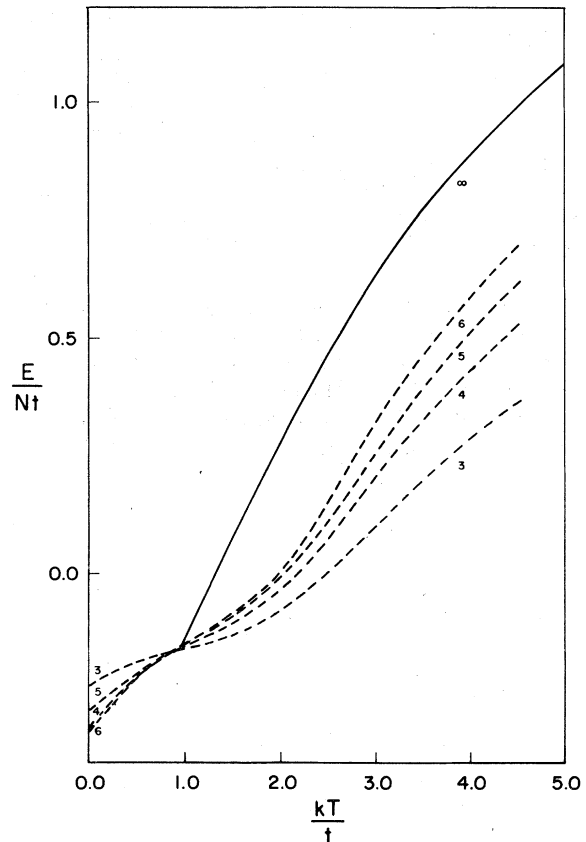


FIG. 1. Internal energy of the one-dimensional half-filled-band Hubbard model with $U/t=8$. The dashed lines represent Shiba and Pincus results of rings with three to six atoms.

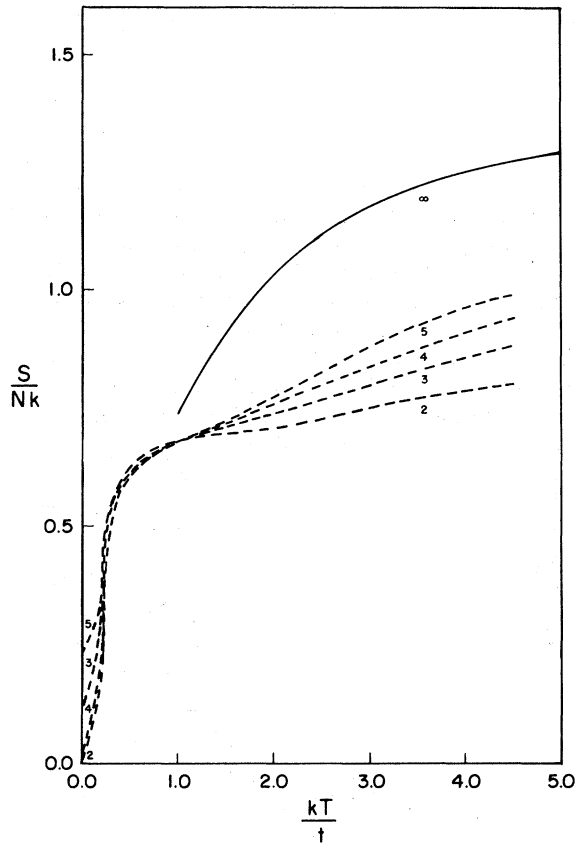


FIG. 2. Entropy of the one-dimensional half-filled-band Hubbard model with $U/t = 8$. The dashed lines represent Shiba and Pincus results of chains with two to five atoms.

rate of convergence of the numerical calculation becomes extremely slow at low temperatures.

Having established the numerical and physical credibility of the present solution, one proceeds to carry out calculations for the three-dimensional half-filled-band Hubbard model in a simple cubic (sc)

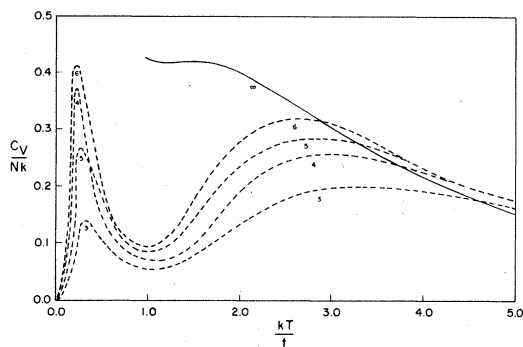


FIG. 3. Specific heat of the one-dimensional half-filled-band Hubbard model with $U/t = 8$. The dashed lines represent Shiba and Pincus results of rings with three to six atoms.

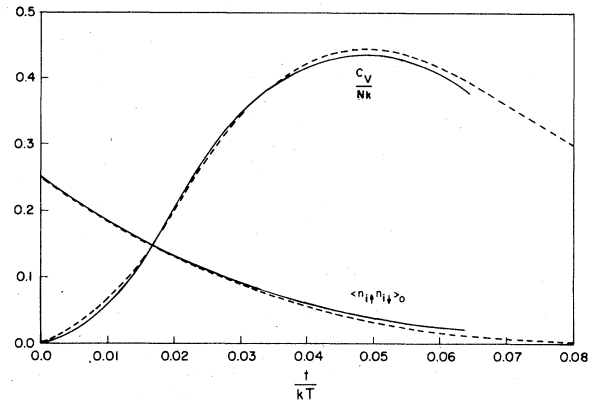


FIG. 4. Specific heat and the probability of double occupancy of the three-dimensional (sc) half-filled-band Hubbard model with $U/t = 100$. The dashed lines are Visscher's results.

structure, i.e., with $q = 6$. The results, some of which include Visscher's data¹⁶ for comparison, are shown in Figs. 4–7. One sees that the specific-heat agreement is very good for large value of U/t (Fig. 4), but not otherwise (Figs. 5 and 6). Visscher did obtain a peak in the specific-heat curve for $U/t = 0.5$ (and possibly one for $U/t = 4$), yet none is resolved in the present calculations. However, in this range of paramagnetic values of U/t , one would expect—as suggested by the one-dimensional results of Shiba and Pincus—only one specific-heat anomaly embodying both the Néel transition and the metal-insulator transition and thus cannot appear in the present solution. Although long-range-ordered antiferromagnetic solutions are excluded from the present solution, one observes from Fig. 5(b) an antiferromagnetic tenden-

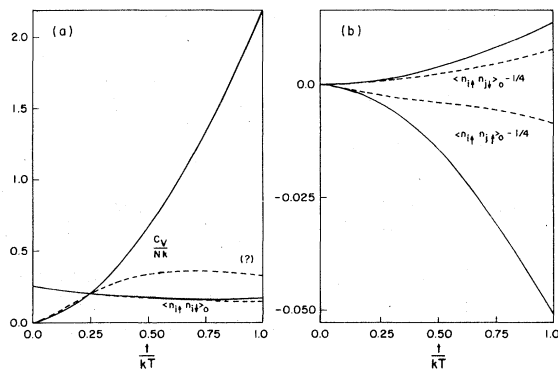


FIG. 5. Three-dimensional (sc) half-filled-band Hubbard model with $U/t = 4$. (a) Specific heat and the probability of double occupancy. The dashed lines are Visscher's results, and the question mark indicates that his data are inconclusive. (b) Short-range (nearest-neighbor) magnetic correlations.

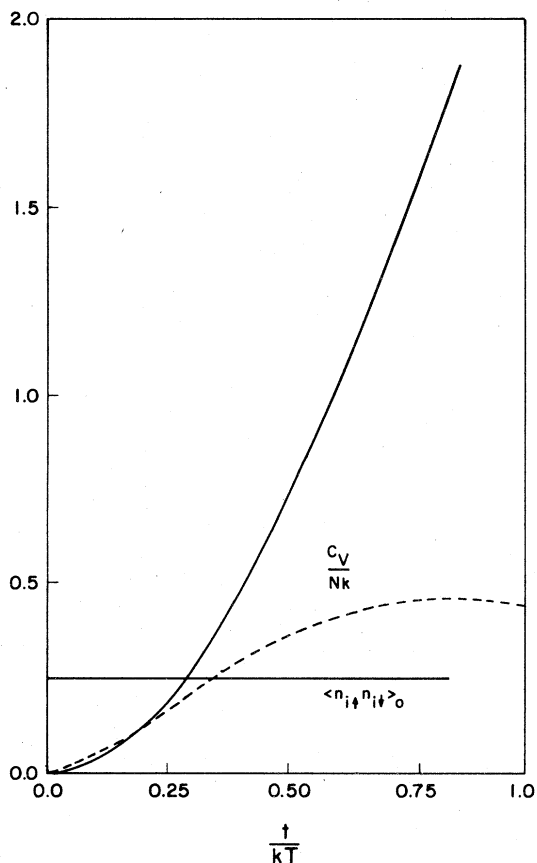


FIG. 6. Specific heat and the probability of double occupancy of the three-dimensional (sc) half-filled-band Hubbard model with $U/t = 0.5$. The dashed line is Visser's result.

cy in the nearest-neighbor magnetic correlations (similar behaviors are observed for other values of U/T). This agrees with the yet unproven but common notion that the three-dimensional half-filled-band Hubbard model also admits an antiferromagnetic ground state.^{21,22} Also similar to the one-dimensional case, a high-temperature peak in the specific-heat curve is found for the three-dimensional sc structure for large enough value of U/t (see Figs. 4 and 7) and it is associated with a gradual metal-insulator transition because of the corresponding decline in the quantity $\langle n_{i\uparrow}n_{i\downarrow} \rangle_0$ (see the discussion at the end of Sec. II).

In contrast to the one-dimensional case, where Shiba and Pincus suggested the two peaks in the specific-heat curve merge at $U/t \approx 4$, the demarcation value of U/t in a three-dimensional (sc) structure is found here to be near 15 (see Fig. 7). Note that the present result is larger than that obtained by Langer *et al.*⁸ (~ 1.08) by an order of magnitude.

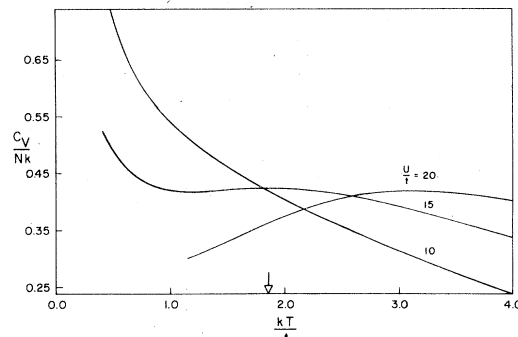


FIG. 7. Specific heat of the three-dimensional (sc) half-filled-band Hubbard model with typical values of U/t around 15. The base arrow indicates the position of the maximum for the case $U/t = 15$.

However, the approximation they employed is less refined than the present two-site cluster approximation which includes four-body correlations, so the present result of $U/t \approx 15$ is probably closer to the actual value.

In conclusion, it has been shown that the cluster variation method in a two-site cluster approximation yields good and consistent results for the half-filled-band Hubbard model. An advantage of using such a method is that the equilibrium correlation values (see, e.g., Fig. 8) are calculated first and these quantities describe the system in a more detailed fashion than the thermodynamic quantities alone. Hence, in this sense, the present results are more complete than those obtained by various other authors.

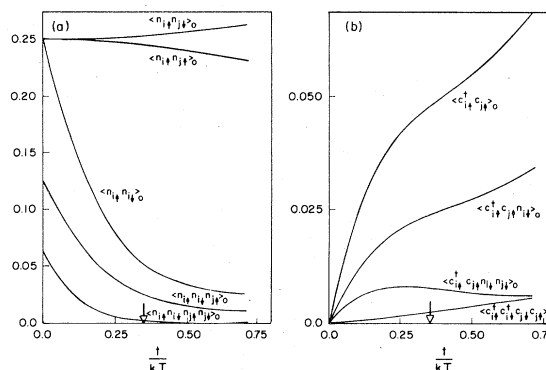


FIG. 8. Equilibrium correlations of the three-dimensional (sc) half-filled-band Hubbard model with $U/t = 15$. (a) $\langle n_{i\uparrow}n_{i\downarrow} \rangle_0$, $\langle n_{i\uparrow}n_{j\uparrow} \rangle_0$, $\langle n_{i\uparrow}n_{j\downarrow} \rangle_0$, $\langle n_{i\uparrow}n_{i\downarrow}n_{j\uparrow} \rangle_0$, $\langle n_{i\uparrow}n_{i\downarrow}n_{j\downarrow} \rangle_0$. (b) $\langle c_{i\uparrow}^\dagger c_{j\uparrow} \rangle_0$, $\langle c_{i\uparrow}^\dagger c_{j\uparrow} n_{i\downarrow} \rangle_0$, $\langle c_{i\uparrow}^\dagger c_{j\uparrow} n_{i\downarrow} n_{j\downarrow} \rangle_0$, $\langle c_{i\uparrow}^\dagger c_{i\downarrow}^\dagger c_{j\uparrow} c_{j\downarrow} \rangle_0$. The base arrow indicates the position of the maximum in the specific-heat curve.

VI. SUMMARY AND DISCUSSION

The cluster variation method in a two-site approximation is applied to the half-filled-band Hubbard model (2). Both the one- and three-dimensional (simple cubic) cases are examined. For sufficiently large value of U/t , a high-temperature peak in the specific heat is seen and is identified as an indication of a gradual metal-insulator transition. For the simple cubic structure, this high-temperature peak disappears as one decreases the value of U/t to around 15. Also, correlation results strongly suggest that the three-dimensional half-filled-band Hubbard model admits an antiferromagnetic ground state.

The present research also opens up some interesting avenues for further investigations. For example, one can ask: What kind of magnetic transition will

take place at low temperatures? Will it be a Néel (continuous) transition or rather a discontinuous one? To answer these questions, one has to solve the entire problem anew by initially assuming the existence of two sublattices and this obviously complicates the diagonalization of the reduced trial density matrix $\rho_T^{(2)}(i,j)$. In fact, one can show that a cubic equation appears in this case, but nonetheless, the problem can be solved theoretically. Finally, it should be pointed out that it is only a matter of computer time to carry out further calculations on the three-dimensional half-filled-band Hubbard model for structures other than simple cubic, for example, the body-centered cubic structure with $q=8$, and the face-centered cubic structure with $q=12$. One can also examine the non-half-filled-band cases by using various values of $\langle n_i \rangle$ other than 1.

APPENDIX A: RIGOROUS CONSTRUCTION OF THE REDUCED TRIAL DENSITY MATRICES

The actual building of the complete one-site reduced trial density matrix $\rho_T^{(1)}(i)$ and the basic mechanics of matrix $[\rho_T^{(2)}(i_1, \dots, i_n)]$ construction has been published,²³ and it was shown that

$$\rho_T^{(1)}(i) = \begin{pmatrix} \langle (1-n_{i\uparrow})(1-n_{i\downarrow}) \rangle & \langle c_{i\uparrow}^\dagger(1-n_{i\downarrow}) \rangle & \langle c_{i\downarrow}^\dagger(1-n_{i\uparrow}) \rangle & \langle c_{i\uparrow}^\dagger c_{i\downarrow}^\dagger \rangle \\ \langle (1-n_{i\downarrow})c_{i\uparrow} \rangle & \langle n_{i\uparrow}(1-n_{i\downarrow}) \rangle & \langle c_{i\downarrow}^\dagger c_{i\uparrow} \rangle & -\langle c_{i\downarrow}^\dagger n_{i\uparrow} \rangle \\ \langle (1-n_{i\uparrow})c_{i\downarrow} \rangle & \langle c_{i\uparrow}^\dagger c_{i\downarrow} \rangle & \langle n_{i\downarrow}(1-n_{i\uparrow}) \rangle & \langle c_{i\uparrow}^\dagger n_{i\downarrow} \rangle \\ \langle c_{i\downarrow} c_{i\uparrow} \rangle & -\langle n_{i\uparrow} c_{i\downarrow} \rangle & \langle n_{i\downarrow} c_{i\uparrow} \rangle & \langle n_{i\uparrow} n_{i\downarrow} \rangle \end{pmatrix}. \quad (\text{A1})$$

For the construction of $\rho_T^{(2)}(i,j)$, the 16 possible states of occupancy are defined in the following order:

$$\begin{aligned} & |00\rangle, c_{j\uparrow}^\dagger |00\rangle, c_{j\downarrow}^\dagger |00\rangle, \\ & c_{j\uparrow}^\dagger c_{j\downarrow}^\dagger |00\rangle, c_{i\uparrow}^\dagger |00\rangle, c_{i\downarrow}^\dagger c_{j\uparrow}^\dagger |00\rangle, \\ & c_{i\uparrow}^\dagger c_{j\downarrow}^\dagger |00\rangle, c_{i\downarrow}^\dagger c_{j\uparrow}^\dagger c_{j\downarrow}^\dagger |00\rangle, \\ & c_{i\uparrow}^\dagger |00\rangle, c_{i\downarrow}^\dagger c_{j\uparrow}^\dagger |00\rangle, c_{i\downarrow}^\dagger c_{j\downarrow}^\dagger |00\rangle, \\ & c_{i\uparrow}^\dagger c_{j\uparrow}^\dagger c_{j\downarrow}^\dagger |00\rangle, c_{i\uparrow}^\dagger c_{i\downarrow}^\dagger |00\rangle, \\ & c_{i\downarrow}^\dagger c_{j\uparrow}^\dagger c_{j\downarrow}^\dagger |00\rangle, c_{i\downarrow}^\dagger c_{i\uparrow}^\dagger c_{j\downarrow}^\dagger |00\rangle, \\ & c_{i\uparrow}^\dagger c_{i\downarrow}^\dagger c_{j\uparrow}^\dagger c_{j\downarrow}^\dagger |00\rangle, \end{aligned}$$

where $|00\rangle$ represents the state with both the i th and j th sites empty.

Note that in the one-site representation,

$$c_{i\uparrow} = c_{j\uparrow} = \begin{pmatrix} 0 & 1 & 0 & 0 \\ 0 & 0 & 0 & 0 \\ 0 & 0 & 0 & 1 \\ 0 & 0 & 0 & 0 \end{pmatrix}, \quad c_{i\downarrow} = c_{j\downarrow} = \begin{pmatrix} 0 & 0 & 1 & 0 \\ 0 & 0 & 0 & -1 \\ 0 & 0 & 0 & 0 \\ 0 & 0 & 0 & 0 \end{pmatrix}.$$

However one can always interpret $c_{i\sigma}$ or $c_{j\sigma}$ as two-

site operators $c_{i\sigma} 1_j$ or $1_i c_{j\sigma}$ where 1_i and 1_j are unit operators on the i th and j th site, respectively, but in the two-site representation these two-site operators should be represented by square matrices of order 16. In this regard, one can show that

$$c_{i\sigma} 1_j = c_{i\sigma} \otimes I_4, \quad 1_i c_{j\sigma} = I_4' \otimes c_{j\sigma}, \quad (\text{A2})$$

where the symbol \otimes stands for direct product,¹⁷ and

$$I_4 = \begin{pmatrix} 1 & 0 & 0 & 0 \\ 0 & 1 & 0 & 0 \\ 0 & 0 & 1 & 0 \\ 0 & 0 & 0 & 1 \end{pmatrix}, \quad I_4' = \begin{pmatrix} 1 & 0 & 0 & 0 \\ 0 & -1 & 0 & 0 \\ 0 & 0 & -1 & 0 \\ 0 & 0 & 0 & 1 \end{pmatrix}.$$

The same rules (A2) are followed in order to represent creation operators. In general, since every two-site operator can be decomposed into a product of creation and destruction operators, the corresponding 16×16 matrices can now be obtained by simple matrix multiplications. For example,

$$\begin{aligned} c_{i\sigma}^\dagger c_{j\sigma} n_{j,-\sigma} &= (c_{i\sigma}^\dagger \otimes I_4) (I_4' \otimes c_{j\sigma}) (I_4' \otimes c_{j,-\sigma}^\dagger) (I_4' \otimes c_{j,-\sigma}) \\ &= [c_{i\sigma}^\dagger (I_4)']^3 \otimes (I_4 c_{j\sigma} c_{j,-\sigma}^\dagger c_{j,-\sigma}) \\ &= (c_{i\sigma}^\dagger I_4') \otimes (c_{j\sigma} n_{j,-\sigma}), \end{aligned}$$

where the following matrix identities have been used:

$$(A \otimes B)(C \otimes D) = (AC) \otimes (BD) ,$$

$$(I_4)^n = \begin{cases} I_4 & \text{for even } n , \\ I_4' & \text{for odd } n . \end{cases}$$

Thus, using direct-product theory, the complete two-site reduced trial density matrix $\rho_T^{(2)}(i,j)$ can be constructed and is displayed in Ref. 24.

APPENDIX B: FERMION ALGEBRA

Since one is considering electronic systems which obey Fermi-Dirac statistics, the basic anticommutation relations are given by

$$\{c_{i\sigma}^\dagger, c_{j\lambda}\} = \delta_{ij} \delta_{\sigma\lambda} , \quad \{c_{i\sigma}^\dagger, c_{j\lambda}^\dagger\} = \{c_{i\sigma}, c_{j\lambda}\} = 0 ,$$

for any i and j ; $\sigma, \lambda = \uparrow$ or \downarrow .

Using the commutator-anticommutator identity

$$\begin{aligned} [AB, C] &= A[B, C] + [A, C]B \\ &= A[B, C] - [A, C]B , \end{aligned}$$

one can easily show that

$$\begin{aligned} n_{i\sigma}^2 &= n_{i\sigma} , \quad [n_{i\sigma}, n_{j\lambda}] = 0 , \\ [n_{i\sigma}, c_{j\lambda}] &= -\delta_{ij} \delta_{\sigma\lambda} c_{i\sigma} , \\ [n_{i\sigma}, c_{j\lambda}^\dagger] &= \delta_{ij} \delta_{\sigma\lambda} c_{i\sigma}^\dagger . \end{aligned}$$

Making use of the latter relations, it is straightforward to prove that, for the Hubbard Hamiltonian (2),

$$\left(\mathcal{H}, \sum_{i=1}^{\pi} n_{i\sigma} \right) = 0 .$$

*Present address: Amoco Production Company, P.O. Box 3092, Houston, Texas 77001.

¹A. H. Wilson, Proc. R. Soc. London Sect. A 133, 458 (1931).

²J. Hubbard, Proc. R. Soc. London Sect. A 276, 238 (1963).

³N. F. Mott, Proc. Phys. Soc. London Sect. A 62, 416 (1949).

⁴E. Lieb and F. Wu, Phys. Rev. Lett. 20, 1445 (1968).

⁵A. A. Ovchinnikov, Sov. Phys. JETP 30, 1160 (1970).

⁶M. Takahashi, Prog. Theor. Phys. (Kyoto) 42, 1098 (1969); 43, 1619 (1970).

⁷See the following and references therein: D. M. Esterling and H. C. Dubin, Phys. Rev. B 6, 4276 (1972); B. H. Brandow, Adv. Phys. 26, 651 (1977); also, *Proceedings of the NATO Advanced Study Institute on Chemistry and Physics of One-Dimensional Metals, Bolzano, Italy, 1976*, edited by Heimo J. Keller (Plenum, New York, 1977).

⁸W. Langer, M. Plischke, and D. Mattis, Phys. Rev. Lett. 23, 1448 (1969).

⁹M. Plischke, J. Stat. Phys. 11, 159 (1974).

¹⁰B. Velický, S. Kirkpatrick, and H. Ehrenreich, Phys. Rev. 175, 747 (1968). J. W. Schweitzer, in *Magnetism in Metals and Metallic Compounds*, edited by Louposzanski, Pekalski, and Przystawa (Plenum, New York, 1976), p. 91.

¹¹J. Halow, T. Tanaka, and T. Morita, Phys. Rev. 175, 680 (1968).

¹²C. C. Chen, Phys. Rev. B 16, 1312 (1977).

¹³C. C. Chen and M. H. Huang, in *Proceedings of the 24th*

Annual Conference on Magnetism and Magnetic Materials, Cleveland, 1978, edited by J. J. Becker and J. C. Bonner, J. Appl. Phys. 50, 1761 (1979).

¹⁴H. Shiba and P. A. Pincus, Phys. Rev. B 5, 1966 (1972).

¹⁵There is some controversy whether the high-temperature state can be properly labeled as a metal. See R. A. Bari and T. A. Kaplan, Phys. Rev. B 6, 4623 (1972).

¹⁶P. B. Visscher, Phys. Rev. B 10, 932 (1974). The authors wish to thank J. W. Schweitzer for this reference.

¹⁷See, for example, E. D. Nering, *Linear Algebra and Matrix Theory* (Wiley, New York, 1963).

¹⁸D. W. Marquardt, J. Soc. Indust. Appl. Math. 11, 431 (1963). J. Campbell, W. E. Moore, and H. Wolf, MIN-MAX, A General Purpose Adaptive Iterator for Nonlinear Problems, Manned Spacecraft Center, NASA, Houston, Texas, 1964 (unpublished).

¹⁹D. C. Mattis and L. F. Landovitz, J. Non-Cryst. Solids 2, 454 (1970).

²⁰The lattice coordination number q is by no means the best indicator of spatial dimensionality. For example, both the three-dimensional simple cubic lattice and the two-dimensional triangular lattice have lattice coordination number $q=6$.

²¹D. R. Penn, Phys. Rev. 142, 350 (1966).

²²Bunli Yang, thesis (University of Illinois, 1973) (unpublished).

²³W. Ho and J. H. Barry, Phys. Rev. B 16, 3172 (1977).

²⁴W. Ho, thesis (Ohio University, 1975) (unpublished).